12th International Congress on the Deterioration and Conservation of Stone
Columbia University, New York, 2012

INFLUENCE OF SALT SOLUTION NATURE ON THE DRYING OF CLAYEY SANDSTONE

Estel Colas[1,2*] and Jean-Didier Mertz[1]
[1] *Laboratoire de Recherche des Monuments Historiques, USR 3224, Champs/Marne, France*
[2] *Université Reims Champagne-Ardenne, GEGENAA, EA 3795, Reims, France*

Abstract

In order to assess durability of potential restoration sandstones for the Strasbourg's cathedral, the petrophysical behaviour of five Triassic siliceous sandstones containing clays was studied. The pore network connectivity plays a decisive role on the kinetic and the distribution of fluid during transfer. In addition, the water retention properties of clay minerals could also affect the fluid transport in porous media, particularly during drying. External conditions influence the decreasing of water content in stones like the temperature, the relative humidity, the presence and force of wind as well as the type of percolation solutions. When salts are dissolved in solution, they can be transported by either diffusion or advection mechanism. During drying, evaporation of saline solutions proceeds as a dynamic process. Indeed the properties of salt solutions are evolving and the appearance of salt crystals alters the paths of salt solutions. Thereby, these processes will determine the resulting distribution of salts in the stone.

In this study, we investigated the influence of external parameters on the drying kinetic of sandstone, ie (i) the wind force effect on the modification of evaporation parameters of stones (drying rate and critical moisture content) and (ii) the nature of the contaminated salt solution (NaCl and Na_2SO_4) for a low concentration of 45 $g.l^{-1}$. Once dried, the salt distribution profiles were quantified by ion chromatography.

Compared to water, the presence of salts in solution drastically reduces the rate of evaporation. Our experimental measurements suggest that the two salts cause the same downward trend of drying kinetics of sandstones whereas the involved transport mechanisms and the resulting salt distribution are different. As a result, NaCl crystallisation causes more pore-clogging than Na_2SO_4, especially for the more macroporous and poor-clayed sandstone facies.

Keywords: sandstones, drying, halite, sodium sulfate, ion chromatography

1. Introduction

Because drying is a key factor for understanding the behaviours of restoration sandstones on monuments, some petrophysical parameters were studied firstly during water evaporation and secondly during salt solutions evaporation.

During water evaporation of porous media, the shrinkage of stones generates a stress field in tension that could be responsible of stone degradation (Jimenez-Gonzalez et al. 2004) because of the lower tensile strength of stones compared to compressive one. In addition, if the percolation solutions are contaminated by soluble salts, their drying lead to the formation of salt crystals in the porous networks.

Salt decay is a complex process in which the physico-chemical characteristics of salts, the hydro-mechanical properties of stone and the external conditions play a role

(Lopez-Acevedo et al. 1997: Rodriguez-Navarro et al. 1999: Steiger et al. and Asmussen 2008).

During drying, the solution flows are conditioned by the external conditions and the stone properties (mineralogy and structure) (Hammecker 1993: Rousset-Tournier 2001). Then, the growth of salt crystals is dependant of the kinetics of formation ie the supersaturation degree as well as the mineralogical and morphological properties of the surface on which it is growing (Correns et al. 1939: Sunagawa 1981: Steiger 2005: Sghaier-Ben Chiekh 2006).

The aims of this study are to evaluate the influence of the environmental conditions (air convection) as well as the nature of solutions (water and salt solutions eg NaCl and Na_2SO_4) on the drying behaviours of clayey sandstones.

2. Materials and method

2.1 Clayey sandstones

Five Buntsandstein sandstones from quarries located in the French and the German part of the Rhenan Basin were studied: the so-called Vosgien and Meules sandstones (Table 1).

These stones are mainly composed of quartz, K-feldspars and micas in clay coatings that represent from 2.9 to 8.9 (w/w). Those clay coatings are all constituted of illite, kaolinite and an interstratified illite/smectite phase (Colas et al. 2011).

The porous networks were investigated by mercury intrusion porosimetry (MIP) using an Autopore IV Micromeritics equipment with a maximum applied pressure of 206 MPa that corresponds to a minimum pore size radius of 3.4 nm. All intrusion curves were significant of unimodal pore size distributions with medium pore radii (MPR) and total porosities respectively ranging from 3.8 to 18.3 µm and from 15.7 to 21.8 per cent (Table 1).

Table 1. Mineralogical and microstructural parameters of the studied sandstones (MPR: medium pore radius). Bj: yellow sandstone from the Bitburg quarry.

Sandstones	**R**	**L**	**G**	**B**	**Bj**
Quarry location	Rothbach (F)	Langensoul-tzbach (F)	Gamburg (G)	Bitburg (G)	Bitburg (G)
Type	Vosgien	Meules	Meules	Meules	Meules
Clay minerals (%)	2.9	7.0	5.9	5.9	8.9
Porosity (%)	21.8	21.1	15.7	18.2	17.6
MPR (µm)	18.3	5.2	3.8	7.5	7.0

2.2 Experimental setup

The typical drying curve could be described by two phases before reaching the stabilisation between the external conditions and the stones (Figure 1). These two phases are representative of different evaporation stages and could be outlined through three parameters:

F: the capillary flow which corresponds to the constant drying rate versus time;

CMC: the critical moisture content corresponds to the residual water content in stone. This relevant parameter denoted the beginning of a transition phase between capillary and diffusion transfer into the porous network;

D: the diffusion coefficient describes the transition phase in which the water flow changes from liquid to gas state *sensu-stricto*. This dual water flow rate is constant versus the square root of time, and is associated with a waterfront recession within the porous network.

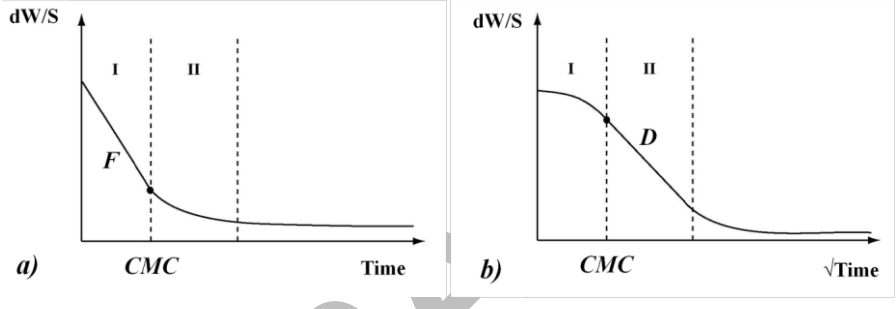

Figure 1. Theoretical description of the macroscopic drying of sandstone: *a)* weight loss versus time; *b*) weight loss versus square root of time.

The drying of sandstones was performed after saturation of the open porosities according to the 48 hours procedure (Hirschwald 1912) on cylindrical cores (40 mm in diameter and 40 mm high). The saturated cores were sealed by plastic films and aluminium tape except on their top faces. The weight loss of sandstones was continuously monitored using a 0.01g balance precision and a 5min step for a total drying period of 70 hours.

In order to simulate the effect of the wind on the drying behaviours of sandstones, a ventilation system was fixed on the desiccator wall. It provides constant air convection into the desiccator that is equal to 0.23±0.02 $m.s^{-1}$ where the samples were located. The isothermal drying of sandstones was performed in the desiccator regulated by a $MgCl_2$ supersaturated solution leading to 33±1% of relative humidity (RH) and a temperature of 22.5±1°C. The presence of air convection enhances the faster RH regulation in the desiccator (Figure 2).

The influence of air convection on the drying behaviour of sandstones was assessed on four samples of each type: two samples without air convection (WA) and two others with air convection (AC).

Afterward, the same samples were contaminated with salt solutions of NaCl and Na_2SO_4 in order to reduce the effect of stone heterogeneities on the evaluation of the combined impact of wind and salts depending of the nature of salt.

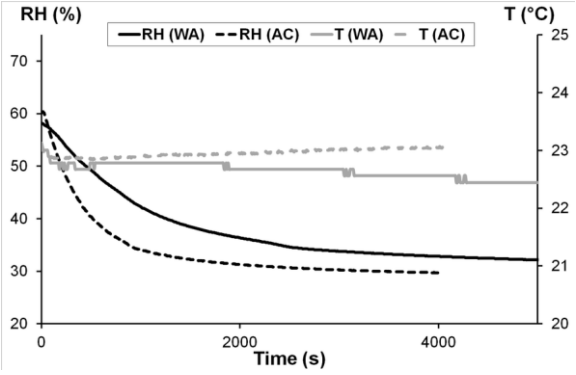

Figure 2. Effect of the air movement on climatic conditions into the drying desiccator: relative humidity (RH) and temperature (T) without air convection (WA) and with air convection (AC).

Previous experimental results on Meules sandstones had been demonstrated that since a 0.18 per cent Na_2SO_4 mass contamination had been exceeded, the alteration occurred (EU SCOST project 2002). Hence, in order to simulate first alteration stages, the salt solutions concentration had been calculated to promote an increasing of 0.25 per cent in mass. Besides the small differences in open porosity from one sandstone to another leading to a range from 36 to 57 $g.l^{-1}$ salt solution concentrations, a medium value of 45 $g.l^{-1}$ of salt concentration has been chosen to focus on sandstones discrimination based on the same intensity of salt solicitation.

After weight loss monitoring, the salt contaminated sandstones were placed under vacuum to preserve the distribution of salt crystals in porous network. The final salt distributions were assessed by ion chromatography (IC) on step drillings along the samples from the stone surfaces.

3. Results and discussion

3.1 Influence of air convection on the drying behaviour of sandstones

The air convection impact on the drying of sandstones could be highlighted by drying parameters and described as (Table 2):

an increase from 2.5 to 2.9 of the capillary flow F;

an increase in CMC value from 20 to 60%;

an increase in diffusion coefficient D from 5 to 50%.

The final water content in stones at the end of the 70 hours weight loss monitoring was closed from one condition to the other.

Regardless of the sandstone type, the large increment in capillary flow confirmed that the flow rate during water evaporation is controlled by dynamic state conditions at the air-stone interface. The increase in capillary flow led to an early rupture of the hydraulic flow observed as an increasing value of CMC. Usually, the more clayey is the sandstone, the higher are the CMC value and the lower the diffusion coefficient D. The hygroscopic properties of clay minerals promoted water retention thus slowing down water transport to the surface during drying. Even though this is not a linear relationship and structure of porous networks had to be considered.

Table 2. Evolution of drying parameters on each type of sandstones without air convection (WA) and with air convection (AC).

		R	L	G	B	Bj
Without air convection (WA)	$F.10^{-3}$ $(g.cm^{-2}.h^{-1})$	17.2 ±2.5	18.1 ±0.1	19.7 ±1.1	18.0 ±2.0	16.5 ±0.4
	CMC (%)	38 ±2	45 ±1	53 ±1	46 ±4	67 ±2
	$D.10^{-2}$ $(g.cm^{-2}.h^{-1/2})$	6.3 ±0.1	5.9 ±0.1	5.5 ±0.1	5.1 ±0.2	5.1 ±0.3
With air convection (AC)	$F.10^{-3}$ $(g.cm^{-2}.h^{-1})$	59.8 ±12.7	62.9 ±0.6	76.3 ±4.1	69.1 ±1.5	79.8 ±8.5
	CMC (%)	60 ±13	63 ±1	76 ±4	69 ±1	80 ±8
	$D.10^{-2}$ $(g.cm^{-2}.h^{-1/2})$	8.8 ±0.2	8.8 ±0.1	6.9 ±0.1	7.2 ±0.2	5.3 ±0.8

The increase in CMC value revealed the bigger proportion of liquid water that fastened the diffusion coefficient D. The CMC and D parameters presented a relationship without air convection that persisted for air convection drying (Figure 3). This relationship is dependant of stone properties. Indeed, the L and R sandstones, which are the more porous and capillary ones, are more prone to be affected by the changes in environmental conditions. On the contrary, the Bj and G sandstones are the less influenced by the presence of air convection because of their low porosities and high clay minerals contents.

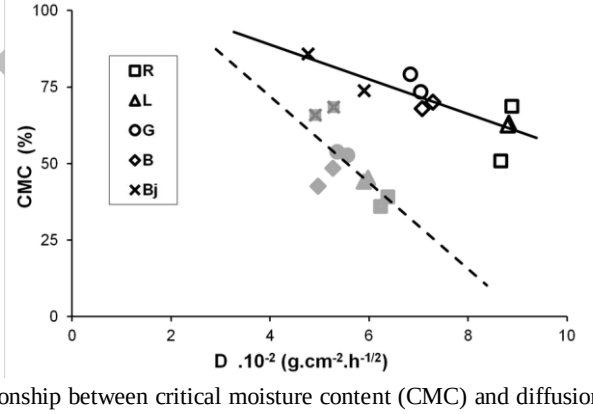

Figure 3. Relationship between critical moisture content (CMC) and diffusion coefficient (D) in absence (WA) or presence (AC) of air convection. (WA: dotted line; AC: continuous line).

3.2 The combined effect of air convection and nature of salt solutions

3.2.1 Sodium Chloride

After NaCl contamination, the drying behaviours of sandstones were significantly

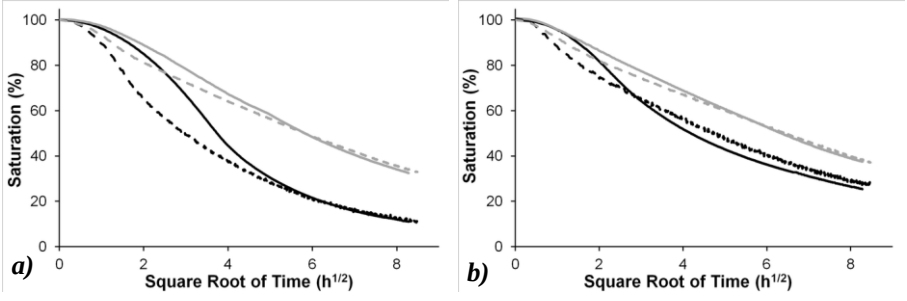

Figure 4. Drying curves of sandstones: *a*) The R Vosgien sandstone; *b*) the Bj Meules sandstone. The black lines represent water evaporation while the grey ones describe NaCl evaporation. The full curves describe the drying without air convection (WA) and the dashed ones for drying with air convection (AC).

altered and showed a decrease in capillary flow rate F, an increase in CMC value and a decrease in diffusion coefficient D (Figure 4).

As a result, a higher final saturation was reached after 70 hours. The presence of air convection enhanced this parameters evolution. The impact of NaCl contaminations could also be observed on the curves shape. The "specific sigmoïd shapes" for water evaporation were flattened for both conditions whatever the type of sandstones. The first capillary stage was drastically shortened before drawing a constant weight loss versus the square root of time until the end of the drying period.

The Cl^- distribution profiles discriminated the sub-surface zone ie from the surface to 12 mm in depth where the anions are concentrated, and the inner zone of stones where the anions contents were stabilized to 0.05 weight per cent of Cl^- (Figure 5). For all type of sandstones, such a distribution of Cl^- content also remained after the drying with air convection.

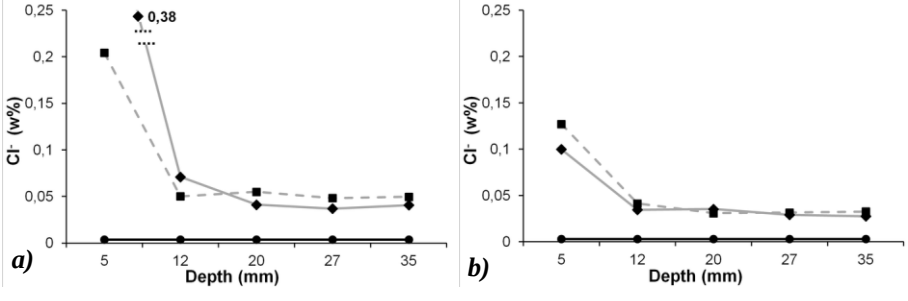

Figure 5. Cl^- distribution profiles determined by IC chromatography along the core samples from the top face to the bottom: *a*) the R Vosgien sandstone; *b*) the Bj Meules sandstone. WA: continuous line; AC: dotted line. Black line corresponds to non-contaminated value.

3.2.2 Sodium Sulfate

The drying of Na_2SO_4 contaminated sandstones showed similar tendencies compared to NaCl contaminated ones. Main changes in the evaporation parameters were related to a decrease in capillary flow F, an increase in CMC value and a decrease in D coefficient.

Nevertheless, for both environmental conditions, the curve shapes showed less intense modifications due to Na_2SO_4 contaminations compared to NaCl ones. Indeed, the sigmoïd curve shape was kept and exhibited a longer first drying phase (Figure 6).

Without air convection (WA), the R and B sandstones presented drying behaviours closed to water drying ones showing the lowest CMC value. This could be related to the higher amount of macropores improving the draining of solutions. Comparing the B and Bj sandstones, which presented almost the same pore size distributions, the higher content of clay minerals in the Bj sandstone inhibited solution transfers to the surface. Hence, the more macroporous and less clayey is the sandstone, the longer is the capillary flow phase of Na_2SO_4 solution without air convection.

With air convection (AC), for the Bj sandstone and to a lesser extent for the B one, the transfer of Na_2SO_4 solution to the surface was promoted. On the contrary, the drying behaviour of the R sandstone was slowed down drastically leading to a higher final content of solution that is characteristic of pore-clogging.

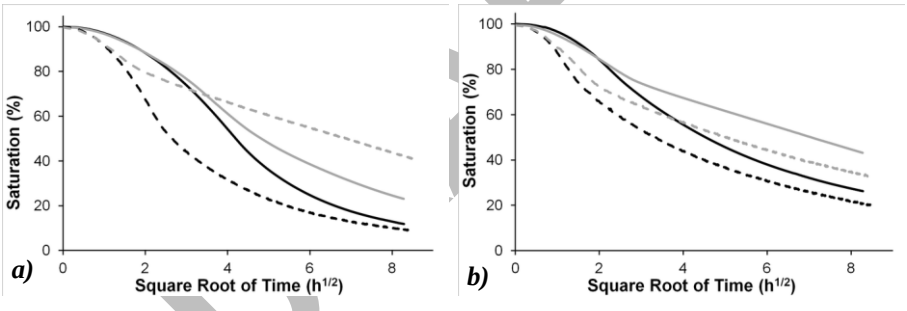

Figure 6. Drying curves of sandstones: *a*) The R Vosgien sandstone; *b*) the Bj Meules sandstone. The black lines represent water evaporation while the grey ones describe Na_2SO_4 evaporation. The full curves describe the drying without air convection (WA) and the dashed ones for drying with air convection (AC).

Compared to Na_2SO_4, the capillary flow F of NaCl contaminated sandstones was increased for both conditions. This fact arises from the differences in equilibrium relative humidity of salts ie RH=75% for halite against 82% for thenardite and 92% for mirabilite at 20°C, compared to distilled water. Hence, the driving force of the solution to flow through the porous material and to reach an equilibrium with the environmental conditions (RH=33%) is lower in the case of NaCl contamination.

After NaCl and Na_2SO_4 salt contaminations, the existing relationship between CMC and D in the case of water evaporation disappeared. Such an evolution could be due to the crystallisation of salts during the second drying phase where D was calculated. This is consistent with the involvement of salt growth in the solution transport even though this peculiar impact is not so easy to define.

Moreover, the lower diffusion coefficient of Na_2SO_4 compared to NaCl could be related to different viscosities for equal mass concentration of salt in solution ie 1.14 Pa.s for Na_2SO_4 against 1.08 Pa.s for NaCl at 45 $g.l^{-1}$ (Handbook of chemistry and physics 1980).

Besides a slightly higher concentration of SO_4^{2-} anions on the sub-surface ie until 12 mm from the top drying surface, the SO_4^{2-} distribution profiles showed localized enrichment or depletion until 20 to 25 mm in depth.

The air convection had a stronger effect on anions localisations of the Na_2SO_4 contaminated sandstones than the NaCl contaminated ones. If air convection is applied during drying, the SO_4^{2-} distribution profiles revealed an enhancement of the salt solution transfer to the surface. However, owing to the pore-clogging effect, the SO_4^{2-} content was significantly increased for the R sandstone (Figure 7).

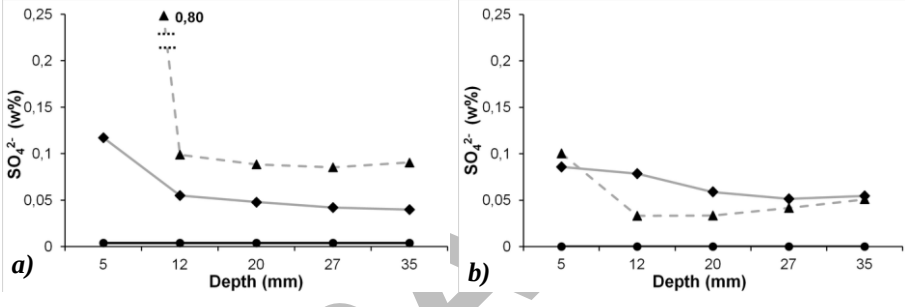

Figure 7. SO_4^{2-} distribution profiles determined by IC chromatography along the core samples from the top face to the bottom: *a*) the R Vosgien sandstone; *b*) the Bj Meules sandstone. WA: continuous line; AC: dotted line. Black line corresponds to non-contaminated value.

8. Conclusions

Experimental simulation of wind was achieved by fixing a ventilator system providing stable air convection inside the climatic chamber. This equipment allowed examining the wind effect on the drying behaviours of sandstones previously saturated with water and salt solutions.

Air convection led to a rising up of the capillary flow F, the critical moisture content CMC as well as the diffusion coefficient D. The higher is the amount of macropores in sandstones, the more influenced by air convection is the drying behaviour. Nevertheless, such an evolution needed to be moderated taking into account the clay content that inhibit the effect of wind because of the hygroscopical properties of sandstones.

After salt contaminations and without any relationship with the air convection conditions, the capillary flow F and the D coefficient were slowed down whereas the CMC value was risen up compared to water transfer.

For all conditions and stone types, the effect of salt contamination was more pronounced after NaCl contamination than Na_2SO_4 one. The capillary phase was drastically shortened and the weight loss curve versus the square root of time turned rapidly as a straight line. This was the case for all drying conditions and sandstone types

revealing a great influence of the NaCl properties on the drying behaviour of sandstones even though the salt solution concentration was moderate. Its great influence was also highlighted by the Cl^- distribution profiles that were concentrated near the subsurface, until 12 mm in depth.

On the contrary, the influence of Na_2SO_4 contaminations was more dependent of stone properties (macropores and clay content) and drying conditions. This could be noticed by the persistence of the sigmoïd curve shape together with the modifications of SO_4^{2-} distribution profiles that showed different local concentrations according to drying conditions and type of sandstones.

Finally, the NaCl contamination caused more pore clogging than the Na_2SO_4 one. Otherwise, the particular R sandstone case revealed that after a faster capillary stage, the Na_2SO_4 crystallisation on the drying face led to a stronger pore clogging compared to NaCl and highlighted by a drastic decrease in drying rate.

References

Colas, E. Mertz, J.D. Thomachot-Schneider, C. et al. 2011. 'Influence of clay coating properties on dilation behavior of sandstones'. In *Applied Clay Science, **5***, 245-252.

Correns, C.W. Steinborn, W. 1939 'Experimente zur Messung und Erklärung der sogennanten Kristallisationkraft'. Zeitschrift für Kristallographie'. In *EU SCOST Project. 2002. Salt Compatibility of Surface Treatments, ENV4-CT98-0710*, **101**: 117-133.

Hammecker, C. 1993. 'Importance des transferts d'eau dans la dégradation des pierres en œuvre'. PhD dissertation, Université Louis Pasteur, Strasbourg.

R. C. Weast, 1981. *Handbook of chemistry and physics.* CRC Press.

Hirschwald, J. 1912. *Die Prüfung der natürlichen Bausteine auf ihre Wetterbeständigkeit.* Berlin: Verlag von Wilhelm Ernst and Sohn.

Jimenez-Gonzalez, I. Scherer, G.W. 2004. 'Effect of swelling inhibitors on the swelling and stress relaxation of clay bearing stones'. In *Environmental Geology*, **46**: 364-377.

Lopez-Acevedo, V. Viedma, C. Gonzalez, V. La Iglesia, A. 1997. 'Salt crystallization in porous construction materials II: Mass transport and crystallization processes'. In *Journal of Crystal Growth*, **182**:103-110.

Rodriguez-Navarro, C. Doehne, E. 1999. "Salt weathering: Influence of evaporation rate, supersaturation and crystallization pattern," In *Earth Surface Processes and Landforms*, **24**: 191–209.

Rousset-Tournier, B. 2001. Transfert par capillarité et évaporation dans des roches- rôle des structures de porosité. PhD dissertation,Université Louis Pasteur, Strasbourg.

Sghaier-Ben-Chiekh, N. 2006. Evaporation en milieu poreux en présence de sel dissous. Influence des films liquides et des conditions de mouillabilité. PhD dissertation, Toulouse: INPT.

Steiger, M. 2005. 'Crystal growth in porous materials I: "The crystallization pressure of large crystals." In *Journal of Crystal Growth*, **282**: 455-469.

Steiger, M. Asmussen, S. 2008. "Crystallization of sodium sulfate phases in porous materials: The phase diagram Na_2SO_4-H_2O and the generation of stress." In *Geochimica et Cosmochimica Acta*, **72**: 4291-4306.

Sunagawa, I. 1981. "Characteristics of crystal growth in nature as seen from the morphology of mineral crystals." In *Bulletin de mineralogy*, **104**: 81-87.